Metal-as-Insulation HTS Insert for Very-High-Field Magnet: A Test Report after Repair

Jung-Bin Song, Xavier Chaud, François Debray, Steffen Krämer, Philippe Fazilleau, and Thibault Lécrevisse

***Abstract*—This study is a sequel to our previous study on a 38 mm diameter cold bore metal-as-insulation (MI) HTS insert that reached 32.5 T in a 18 T background magnetic field. For refurbishing, 7 MI double-pancake (DP) coils were re-wound with used REBCO tapes to just replace the damaged HTS pieces by new ones at inner junctions. 2 DP coils were fully fabricated using new REBCO tapes. The new assembled insert was then tested under various background magnetic fields at 4.2 K. The key focuses of this paper are: 1) the damages in the DP coils; 2) their repair; 3) the characteristics resistance change of the insert; 4) the resistance value of each DP coil; 5) the maximum field of the HTS-resistive hybrid magnet; and 6) the field stability estimation of the hybrid by NMR characterization.**

***Index Terms*— HTS insert, Very-high-field, Metal-as-insulation winding technique, No-insulation, Quench protection**

I. Introduction

FOR quench protection of high-temperature superconducting (HTS) magnets, we have chosen the metal-as-insulation (MI) winding technique by co-winding the bare HTS tape with a metal ribbon which has high electric resistivity and mechanical strength [1],[2]. This winding technique not only utilizes the self-protecting feature of the no-insulated (NI) coil, but also mitigates the charging-discharging delay of NI coils. In addition, mechanical strength of HTS coils is enhanced by the co-wound metal tape [3]-[5]. In 2019, a 38 mm cold bore MI HTS insert developed by two French research institutes (LNCMI-CNRS and DACM-CEA), successfully generated a field of 14.5 T at 322 A (REBCO tape's current density of 716 A/mm^2) in a background magnetic field (B_{ext}) of 18 T, which yields a combined field (B_{tot}) of 32.5 T [6]. However, because this insert experienced two quench events, one because of an unanticipated fault event of the resistive background at B_{tot} = 28 T and the other because of a thermal runaway at B_{tot} = 32.5 T during a field plateau, more than half of the instrumentation channels were lost [6]. To check the HTS insert after those two events, the wiring (mostly voltage taps) and the overbanding (OB) were replaced and the insert tested again up to 300 A in a B_{ext} = 8 T at 4.2 K. Although the MI insert had survived quenches, the total resistance of the insert has increased by an order of magnitude in comparison to the initial experiment. Therefore, in this study, 7 MI double-pancake (DP) coils were re-wound with the former REBCO tapes to just replace the damaged HTS pieces by new ones at the inner junctions. However, 2 DP coils have to be fully fabricated with new REBCO tapes. The repaired DP coils were tested individually in a bath of liquid nitrogen (LN2) at 77 K in self-field (SF) to compare their critical current (I_c), coil constant (α) and electrical resistance values of those they have originally and after being damaged. After assembly of the DP coils, joining and OB, the 9 DP stacked insert was mounted on a newly made probe with a 34 mm bore size tube allowing an access to the center of the coil for further in situ characterizations and future experiments by end users. The insert was tested under various B_{ext} in a bath of liquid helium (LHe) at 4.2 K. The key focuses of this paper are: 1) the damages of DP coils; 2) the repair of DP coils; 3) the characteristics resistance (R_c) change of the MI insert; 4) the electrical resistance (R) value of each DP coil in various B_{ext} at 4.2 K; 5) the maximum center field of the HTS-resistive hybrid magnet; and 6) the field stability estimation of the hybrid magnet by an NMR probe.

Manuscript receipt and acceptance dates will be inserted here. The authors acknowledge the support of the LNCMI-CNRS, member of the European Magnetic Field Laboratory (EMFL), and of the French National Research Agency (ANR) through the contracts ANR-10-LABX-51-01 (Labex LANEF) and ANR-14-CE05-0005 (NOUGAT project). This project has received funding from the European Union's Horizon 2020 research and innovation programme under grant agreement No 951714. *(Corresponding author: Xavier Chaud)*

J. B. Song, X. Chaud, F. Debray and S. Krämer are with LNCMI-EMFL-CNRS, Univ. Grenoble Alpes, INSA, UPS, 38042 Grenoble, France (e-mail: jung-bin.song@lncmi.cnrs.fr; xavier.chaud@lncmi.cnrs.fr; francois.debray@lncmi.cnrs.fr; steffen.kramer@lncmi.cnrs.fr).

P. Fazilleau and T. Lécrevisse are with DACM, IRFU, CEA, Université Paris-Saclay, 91191 Gif sur Yvette, France (e-mail: philippe.fazilleau@cea.fr; thibault.lecrevisse@cea.fr).

Color versions of one or more of the figures in this paper are available online at http://ieeexplore.ieee.org.

Digital Object Identifier will be inserted here upon acceptance.

II. Repair and Experimental set-up

A. Investigation of conductor and joints after two quench events

The I_c, α and R values of each DP coil were measured at 77 K in SF after disassembling the MI insert. The DP coils were unwound and their conductors were closely examined for deformation or burn. Fig. 1 shows the top surface and conductor of DP9 which is the top DP of the insert. As seen in Fig. 1, a wavy pattern formed on the surface of DP9, and the edge part of the conductor was deformed according to this pattern. The height of the winding being 0.2 mm higher than that of the stainless steel (SS) inner ring used as mandrel, this area without mechanical support has been deformed repetitive high magnetic field charging or quenching. Except for DP9 and DP1 located at the top and bottom of the insert respectively, the conductors of the 7 other DP coils were not deformed. To evaluate the damage on conductor of DP9, I_c distribution was measured by Theva using a Tapestar quality control device.

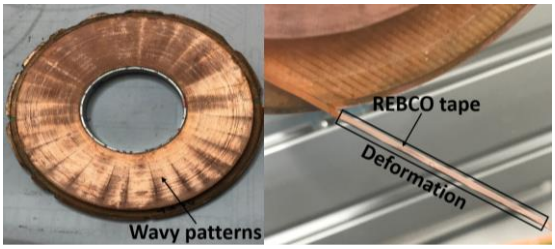

Fig. 1. Photographs of surface and conductor of DP9 after disassembling.

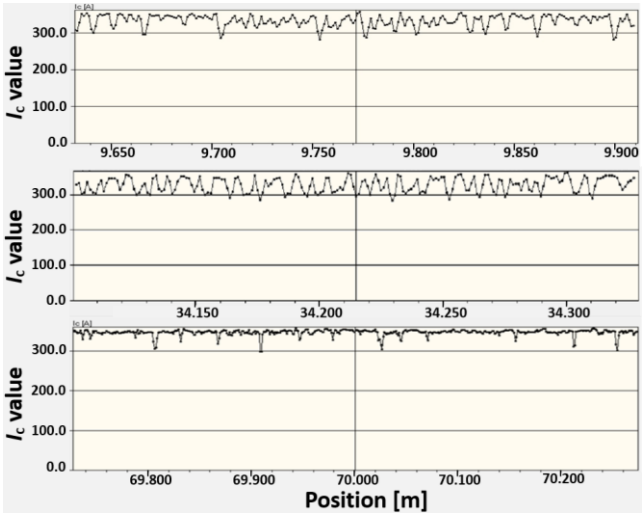

Fig. 2. I_c distribution along the conductor length of DP9 showing regular defects.

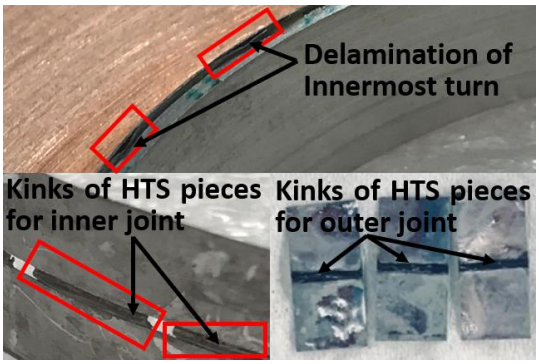

Fig. 3. Photographs of the inner most turn and the kinked HTS joining pieces for inner and outer electrical junctions after two quenches.

Fig. 2 shows the I_c distribution along the conductor length of DP9. The I_c values are regularly degraded at deformed areas by about 15 %. Fig. 3 shows the photographs of the inner most turn (joining area) and the joining pieces of DP coils. The middle part of the HTS joining pieces for inner and outer electrical junctions is kinked due to high magnetic pressures generated by charging and quench events despite uniaxial preloading prior to soldering and the use of Belleville washers. In addition, the inner most turns of the DP coils were delaminated.

To identify the main cause of the high thermal dissipation in the coils, the DP9 was re-wound with used REBCO tape by just replacing damaged HTS pieces by new ones. Table I lists the test results of the original, dismantled and rewound DP9 at 77 K in SF. As seen in Table I, the R and α values of repaired DP9 are of the same order of magnitude as those of original one.

TABLE I. I_c, α AND RESISTANCE VALUES OF DP9 AT 77 K IN SELF-FIELD

		Original	After dismantling	After repairing
I_c (1 μV/cm)	[A]	66.7	65.6	65.5
α at center	[mT/A]	9.3	9.4	9.4
Resistance at 40 A	[nΩ]	375	10800	580

In addition, even if the conductor I_c of dismantled DP9 was degraded due to deformation, the decrease of I_c remains small because a portion of the coil current bypassed the degraded spots and was shared with the nearest turns [7]. It was recently reported that a NI winding with defect cooled by cryocooler is able to be stably operated in 70 ~ 80 % of its estimated I_c value at 20 K [8].

B. Repair, 77 K test and assembly of the MI DP coils

7 DP coils out of a total number of 9 DP coils were re-wound with used REBCO tapes and just the damaged HTS pieces were replaced at inner junctions. Although the repaired DP9 shows electrical resistance close to the original one, because the conductor deformation was obvious and we fear a more severe degradation under high magnetic field, we decided to replace DP9 and DP1 by DPs fully manufactured using brand new REBCO tapes. During repairing process of DP coils, a sapphire plate was inserted for electrical insulation and thermal conduction between the SP coils to enhance the cooling condition inside each DP coil [5]. Fig. 4 shows test results of original, dismantled and repaired MI DP at 77 K in SF. The R values of DP 2~8 with just inner joints replaced were 0.32, 0.17, 0.23, 0.6, 0.33, 0.12 and 0.12 μΩ, respectively. The R values of the DP coils were significantly reduced by making new inner junctions. The nine DP coils were mounted on a support structure and an axial preload pressure of 10 MPa was applied using Belleville washers. For better cooling between DP coils, 0.3 mm thick copper plates insulated by 0.2 mm G-10 sheets, one on each side, were inserted in between DP-DP coils. Each pancake coil was so-called over-banded by about 45 turns of 75 μm thick 316L SS tape. 3 turns of REBCO tape were wound onto the middle of over-banding to eventually reduce induced voltages, currents and unbalance forces generated by quench events. The method of our construction technique for the MI insert has already been described in detail in a previous paper [4]. Table II lists the specifications of the repaired MI insert.

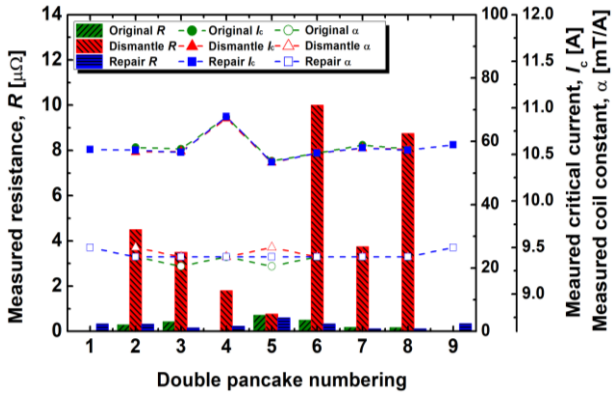

Fig. 4. Measured critical current (I_c), electrical resistance (R) and coil constant (α) of original, dismantled and repaired DP coils at 77 K in self-field.

TABLE II. SPECIFICATIONS OF THE REPAIRED MI HTS INSERT

Parameters		Value
Provider of REBCO tape		SuperPower
REBCO tape width/thickness	[mm]	6/0.075
Inner/outer diameter of DP coils	[mm]	50/110.8
Metal tape for co-winding		Durnomag
Width/thickness of co-winding metal tape	[mm]	6/0.03
Number of turns per SP coils		286
Number of DP coils		9
Outer diameter after stainless-steel OB	[mm]	118.7
Calculated coil constant	[mT/A]	44.3
Magnet inductance (L)	[H]	0.82
Initial characteristic resistance (R_c)	[mΩ]	295
Initial contact surface resistivity	[mΩ·cm^2]	14.7

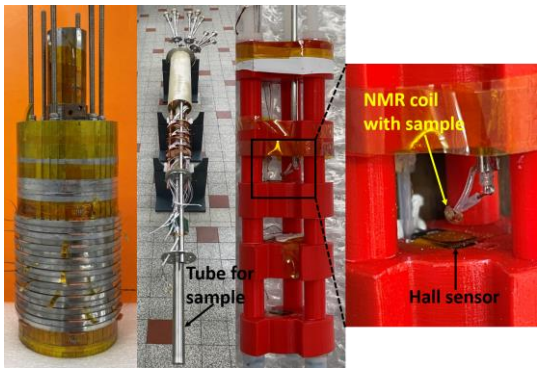

Fig. 5. The photographs of the repaired MI insert, new probe and homemade insert supporting five Hall sensors (Arepoc) and NMR coil with an ^{27}Al sample.

C. New probe and NMR characterization

The MI HTS insert was mounted on a newly made probe with a 34 mm bore size tube to access to its center for NMR characterization and eventually for use by real end-user. To estimate the field stability of the insert, an NMR coil with a 1 mm^3 of ^{27}Al metallic foil sample (gyromagnetic ratio/gamma = 11.1122 MHz/T) as well as some Hall sensors were placed on a support that can be displaced from outside in the 34 mm bore size tube. Fig. 5 shows photographs of the repaired MI insert, new probe and homemade 3D printed support for the Hall sensors and NMR coil. NMR signals were measured under various magnetic fields from 10 T to 28 T. 200 single shot NMR records were taken at each field during 7-8 minutes. All signals but NMR were monitored and simultaneously recorded using a NI cDAQ-9178 chassis comprising several embedded NI-9225, 9229, 9238 and 9239 modules.

III. RESULTS AND DISCUSSION

A. Characteristics resistance change of the MI insert

R_c, the sum of resistances within the NI variant magnets, is mainly dominated by the turn-to-turn contact resistance, which is an important factor in determining the current distribution within the magnets [9]-[19]. Since 2018, we have estimated R_c value of the MI insert by sudden discharge (SD) at low current level (10-20 A) in SF without any specific test interval. In addition, to investigate R_c change with respect to increasing B_{ext}, we also performed this time SD tests from 0 to 15 T. Note that although the screening current induced fields were included in the HTS insert after charging/discharging tests, constant inductance value (0.82 H) of the insert was used for estimation of R_c regardless of existence of them. Fig. 6 shows the measured τ and estimated R_c values in SF at 4.2 K. As seen in this Fig. 6, R_c varies continuously ranging from 185 to 683 mΩ. The initial R_c value of the insert increased probably because the turn-to-turn contact resistivity increased along with the cryogenic work hardening of copper stabilizer under repetitive magnetic pressure load [5], [20]. Meanwhile, after repair, the range of the R_c change is slightly larger but does not deviate significantly.

Left of y-axis in Fig. 7 shows estimated R_c values at B_{ext} = 0, 5, 10, 15 T. The R_c values in SF and 15 T were 185 and 339 mΩ, respectively, indicating that the R_c value increased by 83 %. One of several possibilities for this phenomenon might be the magneto-resistance (MR) of the REBCO tape. MRs of samples prepared in 6 mm × 4 mm size were measured with an alternating current of 5 mA amplitude at 4.0 K. The direction of current and magnetic field applied to the samples are perpendicular and parallel, respectively. For accurate MR measurements, each sample was measured at an optimal frequency that exhibits an in-phase state between output and input phases. Note that AC loss can be negligible because: 1) the directions of magnetic field applied to nonmagnetic samples are parallel; and 2) 5 mA amplitude is quite small to generate AC loss component.

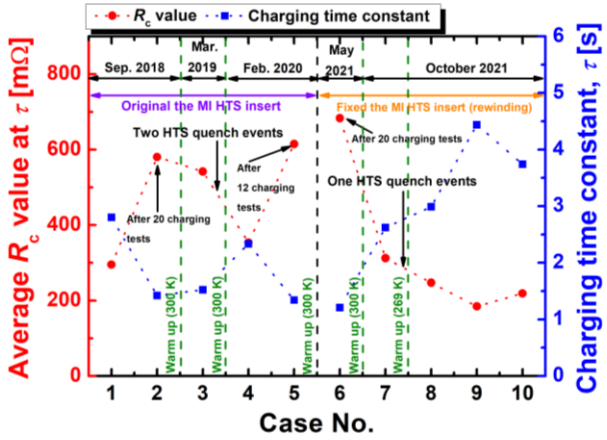

Fig. 6. The measured τ and estimated R_c values of the insert in SF at 4.2 K.

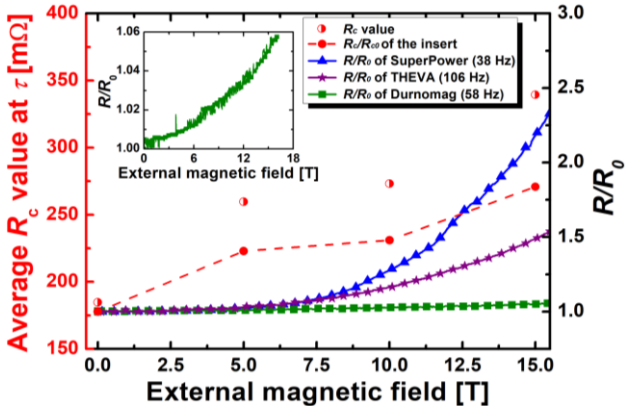

Fig. 7. R_c of the MI insert and normalized magneto-resistance of Durnomag SS tape, THEVA and SuperPower REBCO tapes from B_{ext}= 0 to 15 T.

The right of y-axis in Fig. 7 shows the normalized MR curves as a function of B_{ext} at 4.0 K for the Durnomag tape and, the THEVA and SuperPower REBCO tapes.
The resistance of Durnomag is changing only by a little (4.5 % increase) while the resistances of THEVA and SuperPower REBCO tapes increase from 0 to 15 T by 50 % and 114 %, respectively. This result suggests that the R_c of the REBCO insert is influenced by magneto-resistance.

In sum, because R_c is largely depending on surface condition, contact pressure and intrinsic properties of conductor, it varies continuously by repetitive operations and change of operating conditions. It implies that simulation work using a single value for R_c obtained by SD tests at SF struggles to reflect the reality. Moreover, we also can expect that the local turn-to-turn resistance varies also depending on the position in the coil.

B. In-field resistance value of each MI DP coil

Fig. 8 shows the R value of each DP coil under B_{ext} = 8 and 16 T. All DP coils but DP5 were highly resistive (1.1 ~ 14.1 μΩ) before repair comparing to the original values at the operating current (I_{op}) of 300 A under B_{ext} = 8 T. After repairing the DP coils, they show a much lower R value (210 ~ 520 nΩ) under both B_{ext}= 8 and 16 T except DP7, indicating that most of repaired DP coils are operated well at 4.2 K under very high magnetic field. The damages occurring at quench are mainly localized at the inner and outer electrical junctions made by soldering. The DP coils themselves are well protected by our passive HTS protection scheme comprising the MI winding technique and the over voltage mode of our power supply. We removed the external dump circuit and the breaker prone to create signal spikes. The high electrical resistance at the repaired DP7 occurs because the conductor near the outer junction for a DP-DP junction was damaged during joining process. This damage is localized and can be repaired with sufficient care.

Fig. 9 shows a charging test of the MI HTS insert at a current ramp rate of 0.5 A/s under B_{ext} = 18 T at 4.2 K. The repaired MI insert generated a field of 10.2 T at 235 A under B_{ext} = 18 T, which means a total field strength of 28.2 T as indicated by our central Hall sensor. The coil constants of original and repaired inserts were 44.0 and 43.4 mT/A [5], respectively, implying that there is no by-passing current within the repaired DP coils. Note that the coil constant of the refurbished

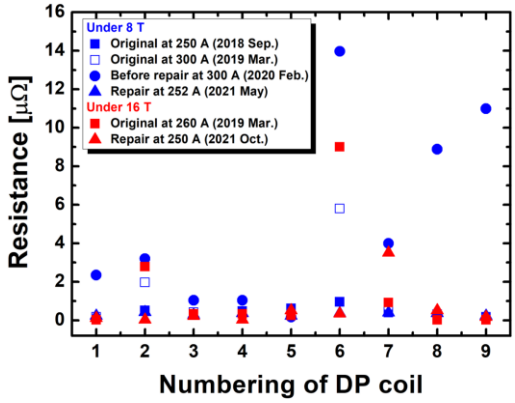

Fig. 8. Electrical resistance values of original, dismantled and repaired DP coils under B_{ext}= 8 and 16 T at 4.2 K.

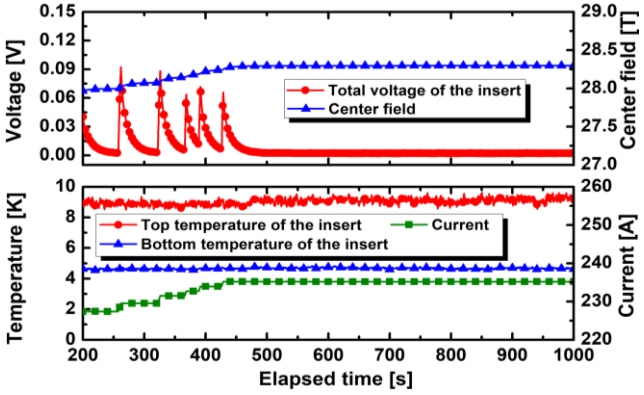

Fig. 9. Charging test results of the repaired MI insert under B_{ext} of 18 T.

insert is slightly smaller than that of original one because a few turns of tapes were removed for repair at the inner and the outer junctions. Some instrumentation wires of the insert suddenly showed abnormal signals like short behavior from 27.7 T. This behavior occurs only at high field and may be linked to an insulation break of our voltage taps when the mechanical pressure increased with the field. It should be noted that at high field, the cooling condition for the repaired insert were more unstable than those for the original one. This might be due to the probe modification letting much less space for liquid helium circulation in the inner bore of the insert because of the additional SS tube. A more stable condition is achieved by pumping on the helium bath. However, the top temperature of the repaired insert increased up to 9 K most probably due to trapped helium bubbles as already observed during other HTS insert tests [20], [21]. Therefore, taking all these issues into account, we decided to stop charging the insert for more higher field.

C. Field stability estimation of the MI insert

Prior to the measurements, the NMR probe was used to determine the magnetic center of the resistive magnet and the HTS insert and to align the coils. The NMR probe is placed at the maximum field. To compare the measurements with Arepoc Hall sensors and NMR characterization, the magnetic field was measured at B_{tot} of 20 T with the background field set to B_{ext}= 10 T at 4.2 K. Fig. 10 shows field stability records measured by a Hall sensor and NMR at B_{tot}=20 T and 4.2 K. The field deviation ($\Delta B/B$) was estimated as follows.

$$\Delta B/B = (B_{measurement} - B_{average})/B_{average} \quad (1)$$

In the case of the NMR measurement, the central magnetic field fluctuation and drift were 5-10 ppm and 5 ppm/min, respectively. Apart from an offset, both measurements agree we start to pump on the helium bath to stabilize the cryogenic condition because the top temperature of the insert was increasing. We observed at this occasion that, as the NMR remained almost stable, the Hall sensor signal is affected by the change of cryogenic condition. Hall records are thus less reliable to estimate the field stability if a change of temperature occurs concurrently. Therefore, the field stability of our resistive-HTS hybrid magnet was only estimated by NMR under high magnetic field.

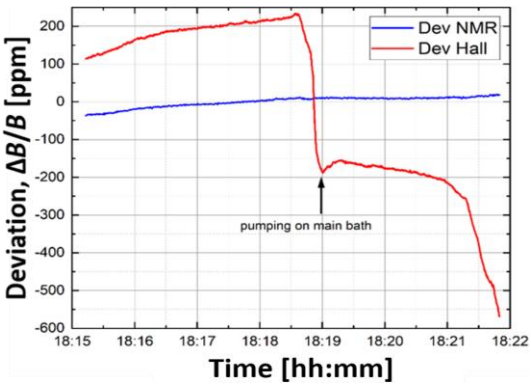

Fig. 10. Time record of field stability measured by Hall sensor and NMR characterization at a total magnetic field of 20 T.

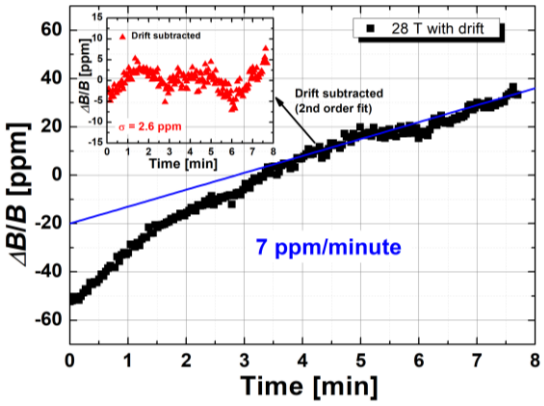

Fig. 11. Field deviation measured by NMR as function of time at a total magnetic field of 28 T at 4.2 K.

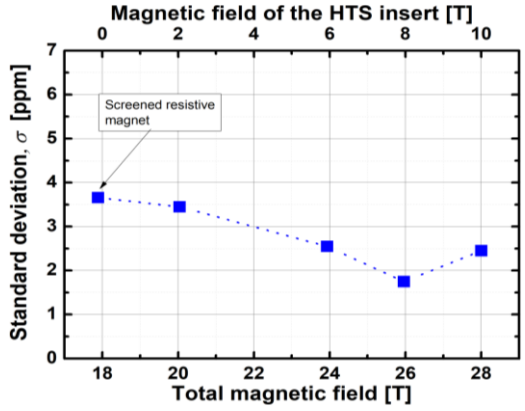

Fig. 12. NMR standard deviation as a function of magnetic field (top axis: HTS contribution, bottom axis: total field) after subtraction of drift term.

Fig. 11 shows $\Delta B/B$ measured by NMR as a function of time at B_{tot}= 28 T at 4.2 K. After 4 minutes, the central magnetic field drift of the hybrid magnet was 7 ppm/min. In addition, the standard deviation (σ) of field fluctuations after subtracting a second order drift term (small figure in Fig. 11) was 2.6 ppm. The field drift of 7 ppm/min is mainly due to magnetic field induced by transient screening currents, as the NMR record started immediately after reaching the target field. Weijers et al. from NHMFL, Tallahassee reported that the central magnetic field drift changed from 10 ppm/min to 0.5 ppm/min (their power supply drift level) after one hour at 32 T [23].

Fig. 12 shows σ of field fluctuation as a function of B_{tot}. σ values of field fluctuation at B_{tot} = 18, 20, 24, 26, and 28 T were 3.65, 3.45, 2.55, 1.75, and 2.45 ppm, respectively, which decreased as the field of the HTS insert increased until B_{tot} = 26 T. At B_{tot} = 28 T, instead of an expected σ decreasing, we observed a higher value. Several factors are involved such as the unstable cryogenic conditions mentioned previously (He bubbles) or the stability of the power supplies.

IV. Conclusion

This paper reports tests of a repaired 38 mm cold bore metal-as-insulation (MI) HTS insert under various background magnetic fields (B_{ext}) at 4.2 K. Based on these test results, the conclusions can be summarized as follows.

1. The characteristics resistance (R_c) value has been continuously changed for 4 years, ranging from 185 to 683 mΩ in self-field (SF) at 4.2 K. In addition, the R_c values increased with increasing B_{ext} probably due to an increase of magneto-resistance. Because R_c is largely depending on surface condition, contact pressure and intrinsic properties of conductor, it varies continuously by repetitive operations and change of operating conditions. It implies that simulation work using a single value for R_c obtained by SD tests at SF struggles to reflect the reality.
2. Electrical resistance (R) of original, dismantled and repaired DP coils replaced by inner joints were estimated at B_{ext} = 8 and 16 T at 4.2 K. All repaired DP coils damaged by outer joining process show low R value under both B_{ext}, which demonstrates that the damages of DP coils were mainly concentrated at inner/outer electrical junctions after two accidental quenches, thanks to our passive HTS protection scheme comprising the MI winding technique and the over voltage mode of power supply.
3. The repaired insert was charged up to 28 T because cryogenic condition was unstable under very high-magnetic field due to trapped helium bubbles and no liquid helium in inner bore of the insert.
4. The resistive and HTS hybrid magnet at 28 T showed good field stability (field drift: 7 ppm/min and standard deviation of field fluctuation: 2.6 ppm), even though it is strongly influenced by some transient screening current induced fields (SCIF) because the NMR record started immediately after reaching the target field. To diminish SCIF effect as much as possible, field stability of the hybrid magnet will be estimated again after staying long time (≥ 1 hour) at target field.

The MI HTS insert will be tested again for the demonstration of 30 T operation.

Acknowledgment

We would like to thank Dr. Benjamin Piot, Dr. Changwoo Cho and Charles Bon-Mardion of MR team in LNCMI for MR measurement and its detailed analysis. We would like also to thank THEVA for I_c distribution measurement and valuable comments. We would like also to thank Rami Nasser Din for assistance for the NMR measurements. We would like also to thank our colleagues Romain Raison and Jürgen Spitznagel for the design and fabrication of our new probe as well as Zeid Louiz for putting all the wiring together.

REFERENCES

[1] T. Lécrevisse and Y. Iwasa, "A(RE)BCO pancake winding with metal-as-insulation," *IEEE. Trans. Appl. Supercond*., vol.26, no. 3, p. 4700405, Jun. 2016.

[2] T. Lécrevisse, A. Badel, T. Benkel, X. Chaud, P. Fazilleau, and P. Tixado, "Metal-as-insulation variant of no-insulation HTS winding technique: pancake tests under high background magnetic field and high current at 4.2 K," *Supercond. Sci. Technol.*, vol. 31, no. 5, p. 055008, Apr. 2018.

[3] P. Fazilleau, B. Borgnic, X. Chaud, F. Debray, T. Lécrevisse, and J. B. Song, "Metal-as-insulation sub-scale prototype tests under a high background magnetic field," *Supercond. Sci. Technol.* vol. 31, no. 9, p. 095003, Jul. 2018.

[4] J. B. Song, X. Chaud, B. Borgnic, F. Debray, P. Fazilleau, and T. Lécrevisse, "Construction and test of a 7 T metal-as-insulation HTS insert under a 20 T high background magnetic field at 4.2 K," *IEEE Trans. Appl. Supercond.*, vol. 29, No. 5, p. 4601705, Aug. 2019.

[5] J. B. Song, X. Chaud, B. Borgnic, F. Debray, P. Fazilleau, and T. Lécrevisse, "Thermal and electrical behaviors of an MI HTS insert comprised of THEVA-SuperPower coils under high background magnetic fields at 4.2 K," *IEEE Trans. Appl. Supercond.*, vol. 30, No. 4, p. 4701806, June 2020.

[6] P. Fazilleau, X. Chaud, F. Debray, T. Lécrevisse, and J. B. Song, "38 mm diameter cold bore metal-as-insulation HTS insert reached 32.5 T in a background magnetic field generated by resistive magnet," *Cryogenics*, vol. 106, p. 103053, Feb. 2020.

[7] S. Hahn, K. Radcliff, K. L. Kim, S. H. Kim, X. Hu, K. M. Kim, D. V. Abraimov, and J. Jaroszynski, "Defect-irrelevant behavior of a no-insulation pancake coil wound with REBCO tapes containing multiple defects," *Supercond. Sci. Technol.*, vol. 29, p. 105017, Sept. 2016.

[8] U. Bong, J. M. Kim, J. S. Bang, J. H. Park, K. J. Han, and S. Hahn, "Defect-irrelevant-winding No-insulation (RE)$Ba_2Cu_3O_{7-x}$ pancake coil in conduction-cooling operation," *Supercond. Sci. Technol.*, vol. 34, p. 085003, June. 2021.

[9] X. Wang, S. Hahn, Y. Kim, J. Bascuñán, J. Voccio, H. G. Lee, and Y. Iwasa, "Turn-to-turn contact characteristics for an equivalent circuit model of no-insulation ReBCO pancake coil," *Supercond. Sci. Technol.*, vol. 26, No. 3, p. 035012, Mar. 2013.

[10] S. Hahn, D. K. Park, J. Bascuñán, and Y. Iwasa, "HTS pancake coils without turn-to-turn insulation," *IEEE Trans. Appl. Supercond*., vol. 21, no. 3, pp. 1592–1595, Jun. 2011.

[11] J. B. Song, S. Hahn, Y. Kim, J. Voccio, J. Ling, J. Bascuñán, H. G. Lee, and Y. Iwasa, "HTS Wind Power Generator: Electromagnetic force between no-insulation and insulation coils under time-varying conditions," *IEEE. Trans. Appl. Supercond.*, vol.24, no. 3, p. 5201005, Jun. 2014.

[12] D. H. Kang, K. L. Kim, Y. G. Kim, Y. J. Kim, Y. J. Park, W. J. Kim, S. H. Kim, and H. G. Lee, "Investigation of thermal and electrical stabilities of a GdBCO coil using grease as an insulation material for practical superconducting applications," *Rev. Sci. Instrum.* vol. 85, no. 9, p. 094701, Sep. 2014

[13] J. B. Song, S. Hahn, T. Lécrevisse, J. Voccio, J. Bascuñán, and Y. Iwasa, "Over-current quench test and self-protecting behavior of a 7 T/78 mm multi-width no-insulation REBCO magnet at 4.2 K," *Supercond. Sci. Technol.* vol. 28, p. 114001, Sep. 2015.

[14] S. Yoon, J. Kim, K. Cheon, H. Lee, S. Hahn, and S. Moon, "26 T 35 mm all-GdBa2Cu3O7–x multi-width no-insulation superconducting magnet," *Supercond. Sci. Technol.*, vol. 29, No. 4, p. 04LT04, March. 2016.

[15] J. Y. Jang, S. Yoon, S. Hahn, Y. J. Hwang, J. Kim, K. H. Shin, K. Cheon, K. Kim, S. In, Y. Hong, H. Yeom, H. Lee, S. Moon, and S. Lee, "Design, construction and 13 K conduction-cooled operation of a 3 T 100 mm stainless steel cladding all-REBCO magnet," Supercond. Sci. Technol. vol. 30, p. 105012, Sep. 2017.

[16] D. Park, J. Bascuñán, P. Michael, J. Lee, S. Hahn, and Y. Iwasa, "Construction and test results of coils 2 and 3 of a 3-nested-coil 800-MHz REBCO insert for the MIT 1.3 GHz LTS/HTS NMR magnet", *IEEE. Trans. Appl. Supercond*., vol.28, no. 3, p. 4300205, April 2018.

[17] M. Wang, Z. Li, J. Jiang, F. Dong, X. Xu, Z. Jin, and K. Ryu, "Performance study on the no-insulation HTS coil wound with narrow-stacked wire", *IEEE Trans. Appl. Supercond.*, vol. 30, No. 4, p. 4703505, June 2020.

[18] J. M. Kim, Y. Kim, S. W. Yoon, K. Shin, J. H. Lee, J. S. Lee, J. T. Lee, J. G. Kim, D. Kim, J. Yoo, H. Lee, S. H. Moon, and S. Hahn, "Design, construction, and operation of an 18 T 70 mm no-insulation (RE)$Ba_2Cu_3O_{7-x}$ magnet for an axion haloscope experiment," *Rev. Sci. Instrum.* vol. 91, p. 023314, Feb. 2020.

[19] Y. Liu, J. Ou, R. Gyuraki, F. Schreiner, W. T-B. Sousa, M. Noe, F. Grilli, "Study of contact resistivity of a no-insulation superconducting coil," *Supercond. Sci. Technol*. vol. 34, p. 1035009, Jan. 2021.

[20] J. Lu, R. Goddard, K. Han, and S. Hahn, "Contact resistance between two REBCO tapes under load and load cycles." *Supercond. Sci. Technol.* vol. 30, p. 045005, Feb. 2017.

[21] U. Trociewitz, M. Dalban-Canassy, M. Hannion, D. K. Hilton, J. Jaroszynski, P. Noyes, Y. Viouchkov, H. W. Weijers, and D. C. Larbalestier, "35.4 T field generated using a layerwound superconducting coil made of (RE)$Ba_2Cu_3O_{7-x}$ (RE = rare earth) coated conductor," *Appl. Phys. Lett.*, vol. 99, p. 202506, Nov. 2011.

[22] H. Bai, S. T. Hannahs, W. D. Markiewicz, and H. W. Weijers, "Helium gas bubble trapped in liquid helium in high magnetic field," *Appl. Phys. Lett.*, vol. 104, p. 133511, Nov. 2014.

[23] H.W. Weijers, "The 32 T superconducting magnet at the NHMFL," *Workshop on State-of-the-Art in High Field Accelerator Magnets*, online, April 16, 2021. Available: https://indico.cern.ch/event/1012691/contributions/4291301/attachments/2227693/3773982/SoftA, Accessed on: Nov. 19, 2021.